PETROLOGY OF UNIQUE ACHONDRITE LEWIS CLIFF 86010. G. McKay (SN4, NASA-JSC, Houston, TX 77058), D. Lindstrom, S.-R. Yang, and J. Wagstaff (Lockheed EMSCO, 2400 NASA Rd. 1, Houston, TX 77058)

Introduction. Preliminary examination of antarctic meteorite LEW 86010 by Mason [1] indicated the unusual nature of this sample. Mason described it as a unique achondrite, with mineralogical and chemical affinities to Angra Dos Reis (ADOR). To further characterize the sample, we performed optical and backscattered electron petrographic investigations and electron microprobe chemical analyses on polished thin section LEW 86010,6. In addition, we collaborated with the Washington University ion probe group to measure REE contents of the minerals in this sample, and to correlate these with major element compositions [2]. Moreover, in a companion abstract [3] we report preliminary results of experimental crystallization studies undertaken to further constrain the petrogenesis of LEW 86010.

General Description. LEW 86010 has hypidiomorphic-granular texture. It consists primarily of euhedral to subhedral plagioclase up to ~2.5mm in size, anhedral to subhedral olivine up to ~1.5mm in size, and anhedral pyroxene grains in clusters up to ~2mm in size. Textural relationships suggest olivine and plagioclase cyrstallized before pyroxene. X-ray identification of 1500 points on a 0.2x0.2 mm grid yielded a mode of 43.3% pyroxene, 31.8% plagioclase, 20.3% olivine, 3.2% kirschsteinite, 0.7% troilite, 0.3% whitlockite, and 0.1% hercynite. Troilite contains rare blebs of Fe metal. A single grain of titanian magnetite was observed, with composition similar to that reported in ADOR by [4]. A portion of the section was discontinuously rimmed with fusion crust.

Mineral Compositions. Fassaitic **clinopyroxene** occurs as anhedral grains or clusters which exhibit spatially irregular zoning of major, minor, and trace elements, often unrelated to obvious grain boundaries. Figure 1 shows pyroxene compositions projected onto the quadrilateral from all other components, and Figs. 2-6 show variation of minor elements. Solid circles are points analyzed for REE [2], and shaded open circles are other points. Also shown are our analyses of ADOR, and, for Na and Mn, of Shergotty. In the projection of Fig. 1, pyroxenes from both LEW 86010 and ADOR lie above the quadrilateral as a result of their large CaTs contents. LEW 86010 pyroxenes show a positive correlation of Ti and Al and a negative correlation of Cr with Fe/Mg. Ti is also highly correlated with Al. Trends for Ti, Al, and Cr show a significant spread at intermediate values of Fe/Mg, but converge to much smaller ranges at low and high Fe/Mg. In all six plots, pyroxenes from LEW 86010 show a much larger variation in chemical composition than those from ADOR. Moreover, ADOR pyroxenes lie distinctly off the trends defined by LEW 86010.

Olivine occurs as subhedral to anhedral crystals of nearly constant Fe/Mg. Spectacular exsolution lamellae of **kirschsteinite** up to 20 um in width occur throughout the olivine at spacings of a few hundred um. In addition, patches of primary kirschsteinite form discontinuous rims around some olivine grains, and themselves contain exsolution lamellae of olivine. Slight but distinct gradients in Fe, Mg, and Ca were observed adjacent to exsolution lamellae in both minerals, and were undoubtedly formed by diffusion during exsolution. Average Fe/Mg of olivine and kirschsteinite are shown in Fig. 1, along with those from ADOR. Both phases in LEW 86010 are less magnesian than either phase in ADOR.

Plagioclase occurs primarily as large subhedral to euhedral grains, but occasionally as rounded inclusions in olivine or, less frequently, pyroxene. Because plagioclase is very low in Na (typically <0.04 wt %), a systematic investigation of plagioclase zoning was not undertaken. However, large grain-to-grain variations in REE content [2] suggest that minor element and Na zoning should be more carefully studied.

Merrillite occurs in only one area of LEW 86010,6, as interstitial grains ~100um in size. Merrillite is depleted in Na by ~2x relative to ADOR, despite being highly enriched in REE.

Analyses of titanian **magnetite** require the majority of Fe to be trivalent to achieve stoichiometry. In contrast, the presence of Fe metal and the small amount of trivalent Fe indicated by hercynite analyses suggest formation under much more reducing conditions than magnetite. We believe it unlikely that the magnetite is primary. Its most probable source is from terrestrial weathering, although pre-terrestrial oxidation cannot be ruled out.

Average mineral compositions are given in Table 1. Because all phases except pyroxene are relatively unzoned for major elements, averages for those minerals should be fairly representative. However, pyroxene is strongly zoned, and thus its average (based on 100 points) may be slightly non-representative. A bulk composition was computed from the mode and average mineral compositions. This composition is probably fairly representative of the section except for the uncertainty associated with the pyroxene average. However, because of the very heterogeneous distribution of merrillite, the P concentration of the bulk sample is subject to a large uncertainty.

Discussion. There is no doubt that LEW 86010 formed by igneous processes. However, is not clear from the texture whether the sample formed through closed system crystallization of a slowly cooled melt, or through

© Lunar and Planetary Institute • Provided by the NASA Astrophysics Data System

crystal accumulation. Experimental studies [3] suggest the presence of slight excess plagioclase and olivine relative to a triply saturated liquid. This observation, together with the texture, suggests to us that the sample may represent melt containing ~10% accumulated plagioclase and olivine. However, it also possible that the sample represents a cumulate of all three major phases, with a relatively small amount of trapped intercumulus melt. Further study is required to discriminate between these possibilities.

The presence of zoning in pyroxene, and its absence in olivine (except for that associated with kirschsteinite exsolution) place qualitative limits on the degree of subsolidus equilibration of LEW 86010. It is clear that LEW 86010 is much less highly equilibrated than ADOR, but lack of zoning in olivine indicates greater equilibration than experienced by typical extrusive basaltic rocks. The spread in pyroxene minor and trace element content at intermediate Fe/Mg may be related to partial homogenization of Fe and Mg during or after crystallization. Future experimental studies may constrain equilibration temperatures, while detailed study of diffusion gradients associated with kirschsteinite exsolution may constrain cooling rates.

Pyroxene Mn content is within uncertainty of that of ADOR, and is much less than that of Shergotty pyroxenes at equivalent Fe content (Fig. 6). Thus, to the extent that pyroxene Mn-Fe relationships are characteristic of parent bodies [e.g., 5,6], LEW 86010 and ADOR appear related. High-sensitivity analyses indicate that LEW 86010 pyroxenes are distinctly depleted in Na relative to ADOR, and that both are highly depleted relative to Shergotty high-Ca pyroxene (Fig. 5). Similar depletions were observed in merrillite. Thus, it appears that LEW 86010 is even more depleted in volatiles than ADOR, which is itself quite volatile-poor.

REFERENCES: [1] Mason (1987) Antarctic Meteorite Newsletter 10, nb2. [2] Crozaz et al. (1988) LPSC XIX, in press. [3] McKay et al. (1988) LPSC XIX, in press. [4] Prinz et al. (1977) EPSL 35, 317. [5] Dymek et al. (1976) GCA 40, 1115. [6] Smith and Hervig (1979) Meteoritics 14, 121.

Table 1. Average phase compositions, mode, and estimated bulk composition (wt.%)

	Mode	SiO_2	TiO_2	Al_2O_3	Cr_2O_3	FeO	Fe_2O_3	MnO	MgO	CaO	S	P_2O_5
Anor.	26.7	43.27	0.01	36.68	0.01	0.23		0.00	0.03	20.54		
Pyro.	44.9	44.56	2.41	9.40	0.26	10.26		0.09	8.60	24.26		
Oliv.	22.9	32.54	0.05	0.03	0.01	50.65		0.62	13.36	2.16		
Kirs.	3.8	32.44	0.04	0.01	0.02	32.21		0.39	4.93	29.22		
Merr.	0.3	0.71	0.01	0.04	0.00	1.62		0.04	2.68	50.68		44.60
Troi.	1.0					61.77					37.60	
Herc.	0.1	0.05	0.78	56.86	1.21	32.24	1.86	0.17	5.87	0.07		
Magn.		0.06	26.98	4.86	1.11	25.78	40.18	0.36	1.16	0.06		
Bulk		40.32	1.10	14.09	0.12	18.24		0.20	7.14	18.20	0.40	0.21

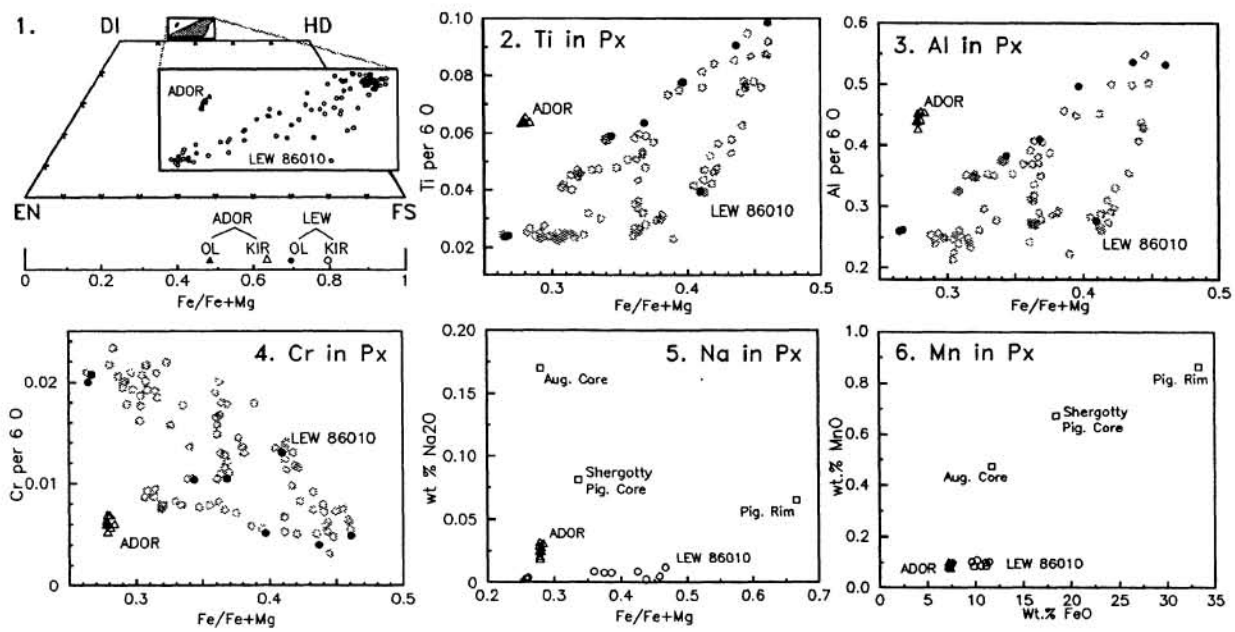

© Lunar and Planetary Institute • Provided by the NASA Astrophysics Data System